J. Physiol. (1981), **311**, *pp.* 289–305
With 8 text-figures
Printed in Great Britain

UNITARY CURRENT THROUGH SODIUM CHANNEL AND ANOMALOUS RECTIFIER CHANNEL ESTIMATED FROM TRANSIENT CURRENT NOISE IN THE TUNICATE EGG

BY HARUNORI OHMORI*

From the Department of Neurophysiology, Institute of Brain Research, School of Medicine, University of Tokyo, Tokyo, Japan

(*Received 30 October 1979*)

SUMMARY

1. The noise included in the Na current and the anomalous rectifier current was measured in intracellularly perfused eggs of *Halocynthia roretzi* Drashe under voltage clamp conditions.

2. The time-dependent component of the point-by-point ratio between the ensemble mean and the variance of successive current traces was the mirror image of the time-dependent component of the mean current itself. This can be explained by assuming an open or closed conductance state for each ionic channel, and permits estimation of unitary currents and channel number.

3. The unitary Na currents showed a potential dependence similar to that of the instantaneous currents. The unitary conductances (γ) at zero membrane potential were 7·4 and 3·3 pmho in sea water with 400 and 100 mM-Na, respectively, and 400 mM-intracellular K. With 400 mM-Na intracellular perfusate and 400 mM-Na sea water, γ was 15·7 pmho. In spite of the large differences in the unitary conductances, the single channel permeability for Na ions remained constant ($1{\cdot}15 \times 10^{-14}$ cm^3 sec^{-1}). The density of Na channels was $0{\cdot}60/\mu m^2$.

4. The unitary currents calculated for the anomalous rectifier showed a potential dependence similar to that of the zero-time extrapolated estimates of the K inward currents. The anomalous rectifier unitary conductance was 5·5 and 6·9 pmho for sea water with 50 and 100 mM-K, respectively. The density of these channels was $0{\cdot}035/\mu m^2$.

INTRODUCTION

Unit conductances of single Na and K channels in the excitable membrane of squid giant axons (Conti, De Felice & Wanke, 1975) and frog myelinated nerve fibres (Conti, Hille, Neumcke, Nonner & Stämpfli, 1976*a*, *b*) are of the order of 10^{-12}–10^{-11} mho. In the undifferentiated membrane of the tunicate egg, the unit conductance of the anomalous K rectifier lies within a similar range as determined by an analysis of steady-state current fluctuations (Ohmori, 1978). Na channels in the tunicate egg membrane are identical to those in other excitable membranes with respect to their kinetic properties and potential dependence (Okamoto, Takahashi & Yoshii, 1976).

* Present address and address for reprint requests: Jerry Lewis Neuromuscular Research Center, School of Medicine, U.C.L.A., CA 90024, U.S.A.

0022-3751/81/2760-0574 $07.50

In view of the universality of ionic channels, it is reasonable to ask whether the unit conductance of Na channels in the egg cell membrane is similar to that of nerve. However, the inactivation of Na currents makes the application of standard methods of steady-state noise analysis difficult.

To circumvent this problem, the ensemble mean and variance calculated from a series of transient Na currents generated at one potential have been analysed by Sigworth (1977) in the node of Ranvier of frog. Both the single Na channel current and the number of operating Na channels can be calculated from the mean current and the current variance within the ensemble. In the present experiments, I measured the unit conductances of Na channels and anomalous rectifier channels of the egg using this method. The value for the anomalous rectifier agrees with the one previously obtained by a different procedure (Ohmori, 1978), supporting the validity of the new method. To reduce the background noise level of the voltage-clamp system, I used low resistance current and potential electrodes which was made possible by an intracellular perfusion technique (Takahashi & Yoshii, 1978).

METHODS

Preparation of eggs and internal perfusion. Unfertilized eggs (mean diameter 270 μm) of the tunicate, *Halocynthia roretzi* Drashe, were used. The preparation of eggs, the control of bath temperature (15 °C), the intracellular perfusion apparatus, and the methods of voltage-clamping were described in a previous paper (Takahashi & Yoshii, 1978). With the perfusion method, the electrode resistances can be less than 1 kΩ, which reduces both the thermal noise level and the potential drift of the electrodes significantly. However, the intracellular perfusion method prevented the exchange of the extracellular medium. Therefore, the extracellular ionic concentration was fixed for each egg during an experiment. The effects of extracellular solutions upon the ionic currents were tested on different eggs. The numerical results are presented as means and standard deviations.

TABLE 1. Composition (mM) of extra- and intracellular solutions

a External solutions

Type	Na	K	Mn	Mg	Choline	Buffer
Ex-A	400	5	10	30	95	10 PIPES*-Na
Ex-B	100	5	10	30	395	10 PIPES-Na
Ex-C	400	50	10	30	50	10 PIPES-K
Ex-D	400	100	10	30	—	10 PIPES-K

b Internal solutions

Type	Na	K	Anion	GEDTA†	PIPES	Glucose	Ca
In-a	—	400	170 F^-	100	20	370	—
In-b	400	—	170 F^-	100	20	370	—
In-c	200	200	170 Cl^-	100	20	370	50‡

* Piperazine-*N*,*N*′-bis[2-ethanesulphonic acid, DOTITE.
† Glycoletherdiamine-*N*,*N*,*N*′,*N*′-tetraacetic acid, DOTITE.
‡ Intracellular free [Ca] is calculated to be 2×10^{-7} M.

Solutions. The solutions used are listed in Table 1. *Extracellular solutions.* Extracellular Ca was replaced with Mn to minimize the contribution of currents through the Ca channel to the total inward currents. The pH was adjusted to 7·0 by 10 mM-PIPES-Na or PIPES-K. *Intracellular*

solutions: F^- solutions (In-*a*, *b*) were the intracellular media used for the analysis of Na currents. The F^- perfusates, however, block the anomalous rectifier completely. Therefore, in the analysis of the current through the anomalous rectifier, a chloride perfusate (In-*c*) was used. To this solution, 200 mM-Na and 2×10^{-7} M-Ca were added, because (1) Hagiwara & Yoshii (1979) reported an increase of the conductance of the anomalous rectifier by intracellular Na, (2) the previous report (Ohmori, 1978) suggested that intracellular free Ca increases the number of anomalous rectifier channels, and (3) an increase in the conductance of the anomalous rectifier was observed at the time of egg activation by the increase of intracellular free Ca (Kozuka & Takahashi, personal communication). The $[Ca]_i$ was adjusted by adding 50 mM-$Ca(OH)_2$ to the 100 mM-GEDTA medium ($K_{Ca}' = 2 \times 10^{-7}$ M, at pH = 7·0). The intracellular pH was adjusted to 7·0 by 20 mM-PIPES-K or PIPES-Na. The extra- and intracellular solutions used are indicated in the Figures as Ext. medium/Int. medium.

Recording and signal processing. The membrane potential was held at -90 mV for the recording of Na currents (solutions Ex-*A*, *B* and In-*a*, *b*), at -30 mV or -20 mV for the recording of K inward currents (solutions Ex-*C*, *D* and In-*c*). The membrane potential was changed stepwise in the positive or negative direction to elicit Na currents or to activate the anomalous rectifier channel, respectively. In the case of internal perfusion with F^--perfusate (In-*a*), the amplitude of Na current (I_{Na}) gradually increased and reached a steady value after several minutes. When the internal perfusate was 400 mM-Na solution (In-*b*), more than 30 min were required for I_{Na} and E_{Na} to settle to a new level. As described by Takahashi & Yoshii (1978), the Na reversal potential (E_{Na}) in 400 mM-Na sea water with 400 mM-Na perfusate is $+6$ mV, which means that the intracellular Na activity is 80 % of the extracellular Na activity.

When the amplitude of Na currents had reached a steady value, the noise analysis or the recording of macroscopic currents was started. The steady-state Na inactivation curve and the instantaneous I–V relation (measured by repolarizing immediately after the peak of inward Na current) were obtained by conventional double-pulse methods. K inward currents through the anomalous rectifier were recorded at different negative membrane potentials.

After recording the macroscopic currents the transient current noise was analysed. The variance of the ionic currents was calculated from a series of current traces. Pulses to one potential level were applied at intervals of 2 sec, which was the minimum time needed to avoid a noticeable depression of Na currents during the train. The currents generated were sampled at a fixed rate (70–500 μsec intervals) by a 12 bit A/D converter, using appropriate amplification and filtering of the high frequency components; single pole, 2-pole and 3-pole low pass Butterworth filters were used in cascade, as described previously (Ohmori, 1978). The minimum cut-off frequency of the filters used in cascade was 0·5, 1 or 2 kHz for Na currents, and 0·2 or 0·5 kHz for K inward currents through the anomalous rectifier. For each experiment, the cut-off frequency of the filters was selected to be close to but less than the Nyquist frequency ($1/2h$) determined by the sampling interval (h) of an A/D) converter (Bendat & Piersol, 1971).

Within one data group consisting of sixteen successive current records the mean and the variance were calculated point-by-point, using a procedure similar to the conventional signal averaging. Estimated means and variances were successively stored on a floppy disk. Four to nine sets of mean and variance records were usually calculated at one potential from the same egg under the same condition. The variance records were in turn averaged and analysed as described in the Results section. Original records of transient currents were also stored on a floppy disk on occasion. When successive currents generated at a potential level failed to superimpose on the storage scope, the series was discarded.

In the regression analysis between the mean current and the variance records, a few sample points during and immediately after the capacitative transient were discarded. These points probably reflect filter-transients and sometimes showed large variances which obscured subsequent time-dependent changes of the variance records. Therefore, data points up to 1–6 msec after the potential step were not analysed. The mean of the variance at four adjacent sample points (indicated by bars in Figs. 2, 3, 6 and 7) was plotted against time, while the ratio between the variance and the mean current was plotted against the mean current at the corresponding time. The regression analysis was made on the plots of the ratio (σ^2/I) against the mean current (I), and unitary currents of Na or anomalous rectifier channels and the number of respective channels in an egg were calculated. Data were recorded and analysed by a PDP-11/03 Labsystem (Digital Equipment Corporation, Maynard, Mass.) and displayed on a Tektronix oscilo-

scope (Model 5113) in X-Y mode. The mean current, the variance record, their ratio and the results of the analysis were plotted by an X-Y recorder (Watanabe Sokki Co., WX-442).

Background noise. The current variances obtained at the holding potential were assumed to originate from thermal background noise of the resting membrane and the recording system. The background variance was subtracted from the test variance before regression analysis. The current variances calculated at various membrane potentials from a series of steady currents obtained after inactivation of the Na current using pulses of longer duration did not show a membrane potential dependence and were similar to the values calculated at the holding potential of -90 mV. The conductance dependence of the background noise (Conti *et al.* 1976*a*) seemed negligible in the egg cell. Depolarizing pulses of long duration frequently caused the membrane to deteriorate. Therefore, the variance calculated at the holding potential was accepted as the background value. This mean background variance was $11{\cdot}27 \times 10^{-22}$ (A^2) for the Na current noise. For the analysis of the anomalous rectifier, the holding potential was equal to the K reversal potential. The mean background variance calculated at this potential was $6{\cdot}43 \times 10^{-22}$ (A^2). It was less than that for the Na current, because the kinetics of the rectifier channel were much slower than those of the Na channel, so that extensive filtering of high frequency components was possible.

RESULTS

Part I. Na channel

Transient current noise of the Na channel. A depolarizing test pulse applied to the tunicate egg cell membrane activates the Na channel (Okamoto *et al.* 1976). The transient Na current was digitized at fixed intervals of 70–200 μsec. Fig. 1*A*, *a* shows inward Na currents recorded successively at -20 mV from a cell perfused with 400 mM-K solution (In-*a*). The mean inward current was calculated within the group (Fig. 1*A*, *b*), and the differences between the mean and each record were calculated on a point-by-point basis (Fig. 1*A*, *c*). The outward Na currents were recorded at $+17$ mV from an egg perfused with 400 mM-Na solution (In-*b*) (Fig. 1*B*, *a*). In this egg the reversal potential of the Na current was $+5$ mV. The mean outward current (Fig. 1*B*, *b*) and the difference between the mean and each original record were calculated similarly (Fig. 1*B*, *c*) These difference currents show fluctuations similar to those in the steady-state current through the Na and K channels (Conti *et al.* 1975, 1976*a*, *b*), the anomalous rectifier (Ohmori, 1978) and the ACh-sensitive end-plate channels (Katz & Miledi, 1972; Anderson & Stevens, 1973).

Fig. 2 shows the mean and the variance records calculated from eighty successive records consisting of five groups for the inward (Fig. 2*A*) and five for the outward Na currents (Fig. 2*B*), both in 400 mM-Na sea water. Both the mean current (I), and the variance (σ^2) show time dependent changes. I and σ^2 follow similar time courses suggesting that the variance records are related to Na current flow. However, as clearly shown in Fig. 2*B*, the peak time of the variance record is different from that of the mean Na current of the ensemble (arrows). If fluctuations of the clamped membrane potential, of the temperature, or of the amount of current through the open-conducting-channels were the main cause of the variance, the variance would follow exactly the same time course as the square of the mean current. Since this is not the case, the variance cannot be entirely due to fluctuations of the parameters which determine the amount of current flow. Sigworth (1977) concluded that these fluctuations originated in the random opening-closing gating kinetics of the Na channel.

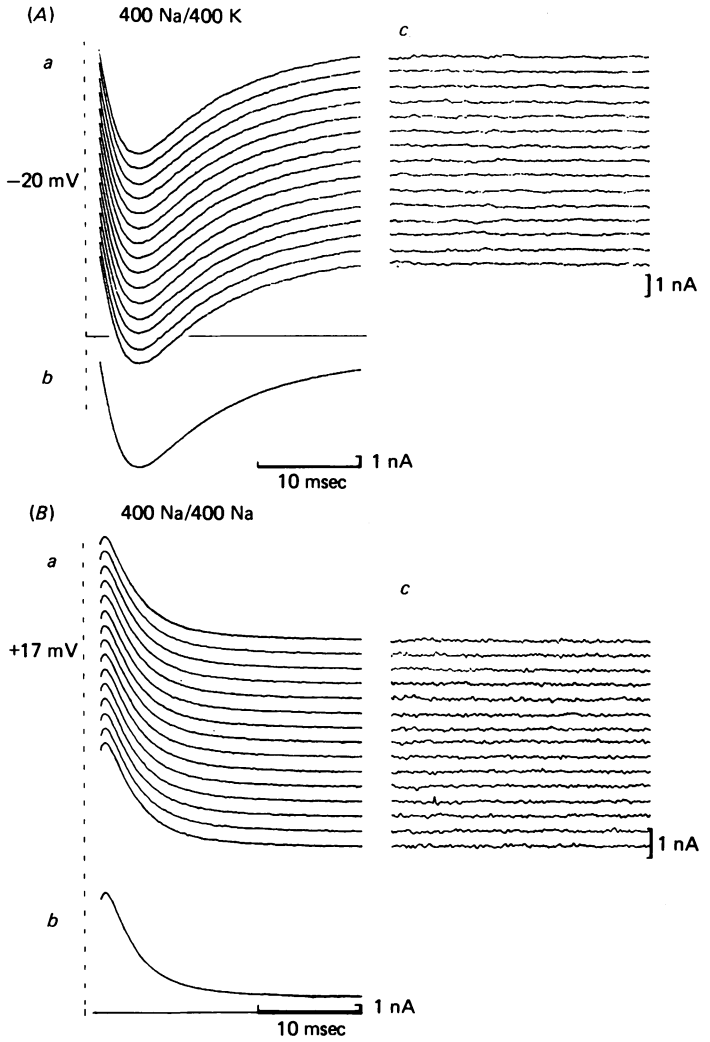

Fig 1. Transient Na current elicited at −20 mV with 400 mM-K intracellular medium (*A*) and at +17 mV with 400 mM-Na intracellular perfusate (*B*); both recorded in 400 mM-Na sea water. Sampling started at 1·4 msec (*A*) and at 1·6 msec (*B*) after the potential step. *a*, original fifteen current traces low-pass filtered at 1 kHz and sampled at 100 μsec intervals. *b*, the point-by-point mean of *a*. *c*, the point-by-point differences between each current trace *a* and the mean ionic current *b*. For the sake of data storage, the sixteenth original traces were replaced by the mean of the current traces. In this and in the following figures, the vertical broken lines indicate the beginning of the potential step. Note the differences in the current calibrations.

Not only Na channels but also voltage-dependent Ca channels exist in the egg cell membrane of the tunicate (Okamoto *et al.* 1976). Both channels are activated by the depolarizing test pulse. However, the intracellular F^- perfusate (In-*a*, *b*) blocks the Ca channel, and the external Mn and Mg ions do not pass through the Ca channel. The contributions of the K outward current or the leakage current to the total membrane current were also negligible in the potential range analysed (Takahashi & Yoshii, 1978). Therefore, the depolarizing test pulses were considered to generate a pure Na current flowing through only the Na channel.

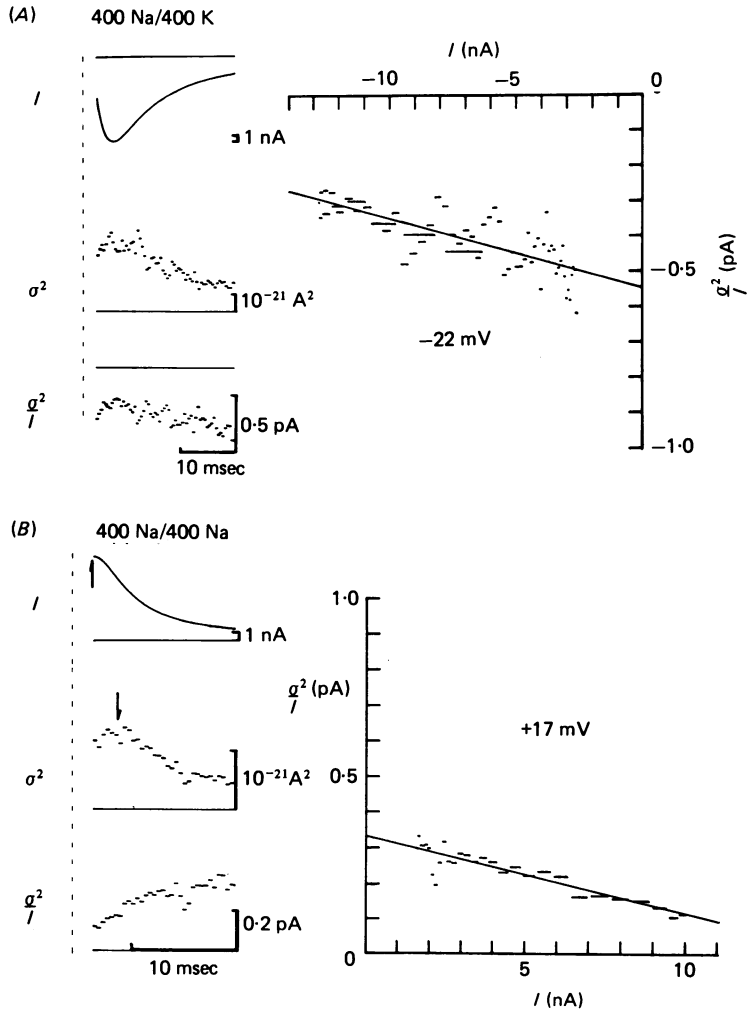

Fig. 2. Mean ionic currents (I), the point-by-point variance (σ^2) of the eighty traces of ionic currents low-pass filtered at 1 kHz and sampled at 100 μsec intervals, and the ratio between σ^2 and I, recorded in 400 mM-Na sea water with 400 mM-K (A) or 400 mM-Na (B) intracellular perfusate. The sampling points during the first 2·3 msec (A) and 2 m sec (B) after the potential step were discarded. The background variance ($5{\cdot}8 \times 10^{-22}$ A^2 for A and $2{\cdot}6 \times 10^{-22}$ A^2 for B) has been subtracted. σ^2 and σ^2/I were calculated as the mean of four adjacent time points. Note that the ratio (σ^2/I) has a time course that is the mirror image of the time-dependent component of the mean current (I). At the right, σ^2/I (Y-axis) was plotted against I (X-axis). The straight line was drawn from a least-squares fit using eqn. (4); the regression coefficient was 0·61 for A and 0·82 for B. The Y-intercept of the regression line indicates the unitary currents: $-0{\cdot}54$ pA in A and $+0{\cdot}33$ pA in B. The reciprocal of the slope permits calculation of the number of channels.

Ensemble variance originated in channel gating. If the transient current noise originated in the random opening-closing kinetics of each Na channel, the time-dependent changes of the variance records can be interpreted in the following way. Let the Na current be the sum of unitary currents which flow through N homogeneous, independent Na channels. As originally assumed by Hodgkin & Huxley (1952), each Na channel has only two states, open or closed. The probability of the open state of each channel at time t after the depolarizing pulse is $p(t)$. Then, by the binomial theorem, the mean Na current and the variance of the current at time t after the depolarizing pulse would be

$$I_{Na}(t) = i\,N\,p(t), \tag{1}$$

$$\sigma_{Na}^2(t) = i^2\,N\,p(t)\,[1-p(t)], \tag{2}$$

where i is the Na current through a single open channel (Neher & Stevens, 1977). Eqns. (1) and (2) yield the relations

$$\sigma_{Na}^2(t)/I_{Na}(t) = i\,[1-p(t)], \tag{3}$$

$$= i - I_{Na}(t)/N. \tag{4}$$

Taking i and N as time-independent parameters, eqn. (4) predicts that the time-dependent component of the ratio between the variance and the mean current (σ^2/I) is the mirror image of the time-dependent component of the mean current itself (I). Fig. 2 shows this. The background variance was subtracted before the calculation of the ratio. Therefore, qualitatively, it seems reasonable that the current noise in the transient Na current originates from random opening and closing of independent unitary Na channels.

Estimation of the unitary current and the number of Na channels. Eqn. (4) also shows that the estimation of the single channel current, i, and the number of operating channels, N, is possible without any knowledge of the stochastic parameter, $p(t)$. When σ^2/I is plotted against the mean current (see Fig. 2, $I-\sigma^2/I$ relation diagram), the Y-intercept of the regression line will be the unitary current, i. From the inverse of the slope, the number of channels, N, can be estimated. The estimated unitary current was $-0{\cdot}54$ pA at -22 mV from Fig. 2*A* and $+0{\cdot}33$ pA at $+17$ mV from Fig. 2*B*. The number of channels estimated was 5×10^4 for Fig. 2*A* and $4{\cdot}4\times10^4$ for Fig. 2*B*.

Fig. 3*A* shows records in 400 mM-Na sea water with 400 mM-K intracellular medium (In-*a*). For this series of regression lines the Y-intercept decreases in magnitude as the potential becomes more positive, but the slope is almost the same for all potentials. Thus, it is clear that the number of channels is independent of the membrane potential. Fig. 3*B* shows records in 100 mM-Na sea water. The slopes of the regression lines were again independent of the membrane potential, and the unitary currents clearly were smaller than those observed in 400 mM-Na sea water. The potential-dependent changes of the unitary current were also observed in 400 mM-Na sea water with 400 mM-Na intracellular perfusate (In-*b*) (Fig. 3*C*). In this case, the slope of the regression lines changed slightly, but showed no simple potential dependence. The mean numbers of channels in each solution are presented in Table 2; the average number of operating channels was $6{\cdot}9\times10^4$.

The number of channels per egg shows a large standard deviation (Table 2). This large standard deviation most probably results from actual differences in channel number between the different egg cells studied, because the peak inward Na current also showed a large standard deviation: $41{\cdot}5 \pm 21{\cdot}9$ nA ($n = 41$) for 400 mM-Na sea water with 400 mM-K intracellular perfusate. This was larger than the standard deviation of the maximum chord conductance of the anomalous rectifier: $3{\cdot}17 \pm 0{\cdot}57$ ($\times 10^{-8}$) mho ($n = 12$) for 100 mM-K sea water. The differences in the effective area of the egg membrane for each intracellular perfusion may also result in variation of N.

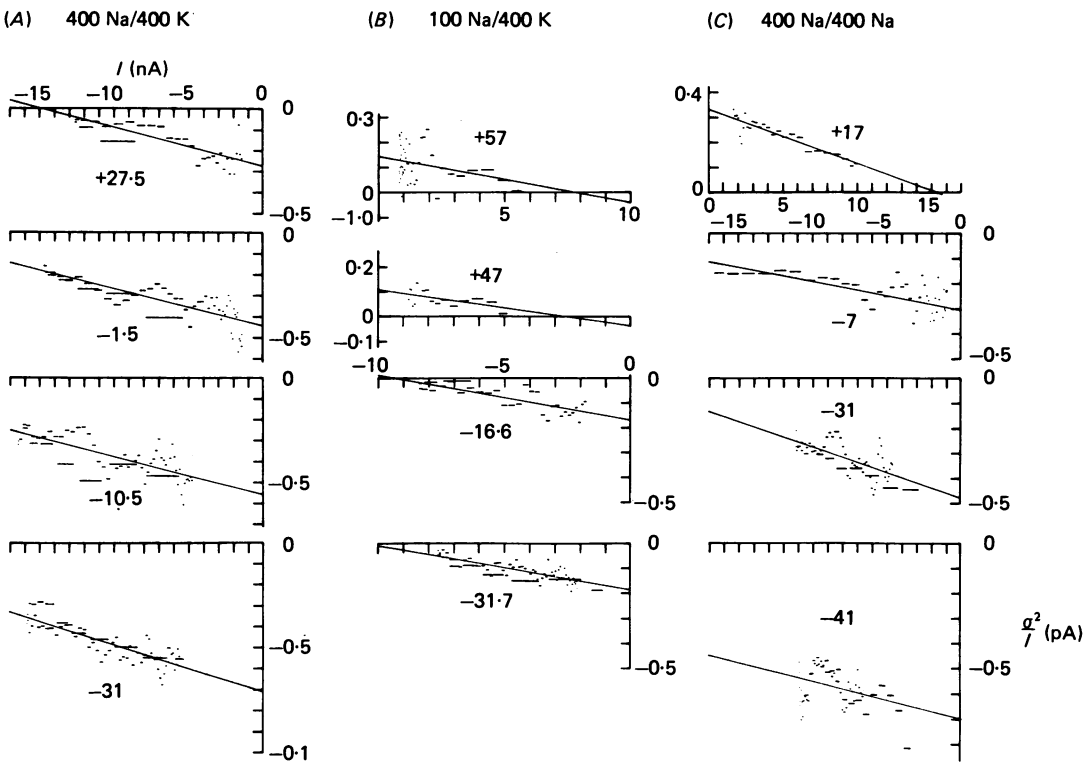

Fig. 3. The ratio of variance to mean Na current was plotted against mean current at the corresponding time, under the experimental conditions indicated as External medium/Internal medium The means and the variances were calculated from 64 to 112 current traces. The current traces were sampled at 70 μsec intervals in B at +47, +57 mV, at 200 μsec intervals in C at −41 mV, and the other records were sampled at 100 μsec intervals. For the sampling at 70, 100, and 200 μsec intervals, the current records were low-pass filtered at 2, 1, and 0·5 kHz respectively. The fitted lines were drawn by the least-squares technique using eqn. (4).

Unitary current– and instantaneous current–voltage relations. The unitary currents were dependent upon the membrane potential, while the number of channels was independent of membrane potential. These results seem consistent with the hypothesis that the transient current noise originates in the gating kinetics of each Na channel.

The instantaneous Na current obtained immediately after a step change of membrane potential at the peak of inward current is considered to be the current which flows through a fixed number of Na channels. Therefore, the membrane-potential-

dependent change of the instantaneous current is a macroscopic indicator of the membrane potential dependence of the Na current through a single Na channel. The insets in Fig. 4 show traces of instantaneous currents in 100 and 400 mM-Na sea water with 400 mM-K intracellular perfusate. After scaling (see legend), the instantaneous currents (.) were plotted against membrane potential in Fig. 4.

The unitary currents estimated above were plotted against the membrane potential on the same axis as the instantaneous currents: △, in 100 mM-Na sea water and ○, in 400 mM-Na sea water with 400 mM-K intracellular perfusate. The unitary currents show a membrane-potential dependence similar to that of the Na current generated by an ensemble of a fixed number of open-Na-channels; both decrease as the membrane potential approaches the Na reversal potential. This strongly suggests that the estimated unitary current corresponds to the current through a single Na channel.

TABLE 2. Microscopic properties of Na channels and anomalous rectifier channels estimated from the transient current noise of intracellularly perfused tunicate eggs (means ± S.D.)

Na currents	N (per half egg)*	γ† (pmho)	($\times 10^{-14}$ cm^3 sec^{-1}) P_{Na}	n	E_{Na} (mV)
400 Na/400 K	77,300 ± 42,200	7·35 ± 1·02	1·15 ± 0·16	60	+53
100 Na/400 K	72,500 ± 49,900	3·26 ± 1·01	1·19 ± 0·37	26	+18·6
400 Na/400 Na	53,700 ± 56,600	15·72 ± 3·42	1·12 ± 0·24	38	+ 5
Averages	69,100	—	1·15	124	—
K inward currents					E_K (mV)
50 K sea water	4100 ± 1100	5·50 ± 0·77	—	35	−34·4
100 K sea water	4000 ± 1000	6·92 ± 0·56	—	32	−17·2
Averages	4050	—	—	67	—

* Because of the intracellular perfusion, the effective surface area of the egg membrane is about half of that of the intact egg (Takahashi & Yoshii, 1978).

† γ values were normalized to zero membrane potential for Na currents. For K inward currents, γ values are the mean of the values calculated at each potential.

Fig. 4 further shows that the unitary conductance depends upon the extracellular Na concentration; the unitary conductance normalized to zero membrane potential was 7·35 pmho in 400 mM-Na and 3·26 pmho in 100 mM-Na sea water (see Table 2). The fourfold decrease in $[Na]_o$ did not produce a proportional decrease in γ_{Na}.

When the intracellular perfusate was changed from 400 mM-K to 400 mM-Na, the unitary currents again showed a potential dependence that paralleled that of the instantaneous currents (Fig. 5). In this case, however, the unitary conductance at zero membrane potential was considerably larger than that with 400 mM-K intracellular perfusate (Table 2).

Na channel permeability. The constant field theory predicts that the current through an ionic channel is determined by the membrane potential, the permeability coefficient, and the concentration of the permeable ionic species on both sides of the membrane. The unitary Na permeabilities (P_{Na}) were calculated from the unitary currents, i, using the constant field equation (Goldman, 1943; Hodgkin & Katz, 1949)

$$i = E \cdot \frac{F^2}{RT} \cdot \frac{P_{Na}[Na]_o - P_C[C]_i \exp(FE/RT)}{1 - \exp(FE/RT)}, \quad (5)$$

where P_C is the unitary permeability for the intracellular cation C (Na or K), E the

membrane potential, $[Na]_o$ the extracellular Na concentration, $[C]_i$ the concentration of intracellular permeable cation C, and F, R and T the usual thermodynamic quantities. When the egg was perfused with K solution (solution In-a), P_{Na} was assumed to be 8·45 times larger than P_K. This ratio was determined from the reversal potential of Na currents presented in Table 2.

Although the unitary Na conductance (γ) showed large differences under different conditions (see Table 2), the unitary permeabilities, P_{Na} (ext. medium/int. medium),

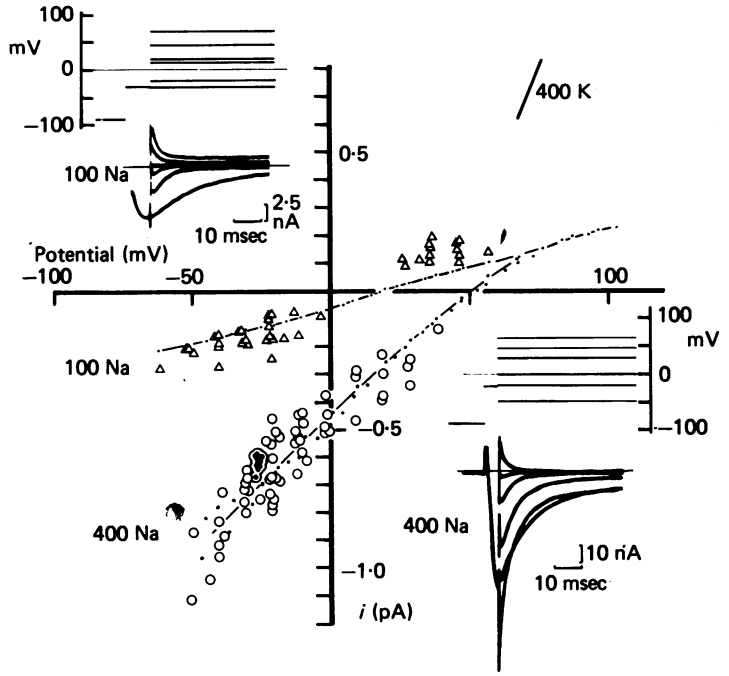

Fig. 4. Unitary currents plotted against membrane potential; △ in 100 mM-Na and ○ in 400 mM-Na sea water with 400 mM-K intracellular perfusate. The enclosed symbols (◎) are the unitary currents obtained with 1 sec prepulses to potentials between −61 and −52·5 mV; the peak inward currents changed 3·2 folds. The insets show traces of instantaneous currents elicited by a step potential change immediately after the inward current peak. The instantaneous currents are plotted as dots (.). Values for 400 mM-Na sea water were obtained from two eggs. The instantaneous currents were multiplied by $2{\cdot}0 \times 10^{-5}$ (one set of the 400 mM-Na records and the 100 mM-Na records) or by $1{\cdot}0 \times 10^{-5}$ (the other set of 400 mM-Na records which are presented in the inset). The scaling factor was determined for each I–V relation so as to give convergence to a single curve at large positive membrane potentials. The reversal potential was +18·6 mV in 100 mM-Na sea water and +53 mV in 400 mM-Na sea water.

were almost constant: P_{Na}(400 Na/400 K): P_{Na}(100 Na/400 K): P_{Na}(400 Na/400 Na) = 1·0 : 1·04 : 0·98. This constancy of the permeability coefficient under various experimental conditions suggests that the current through a single Na channel can be described by the constant field theory.

The mean unitary conductance and permeability in 400 Na/400 K were calculated from the plot in Fig. 4 (from −50·5 to +38·5 mV), while the mean unitary conductance and permeability

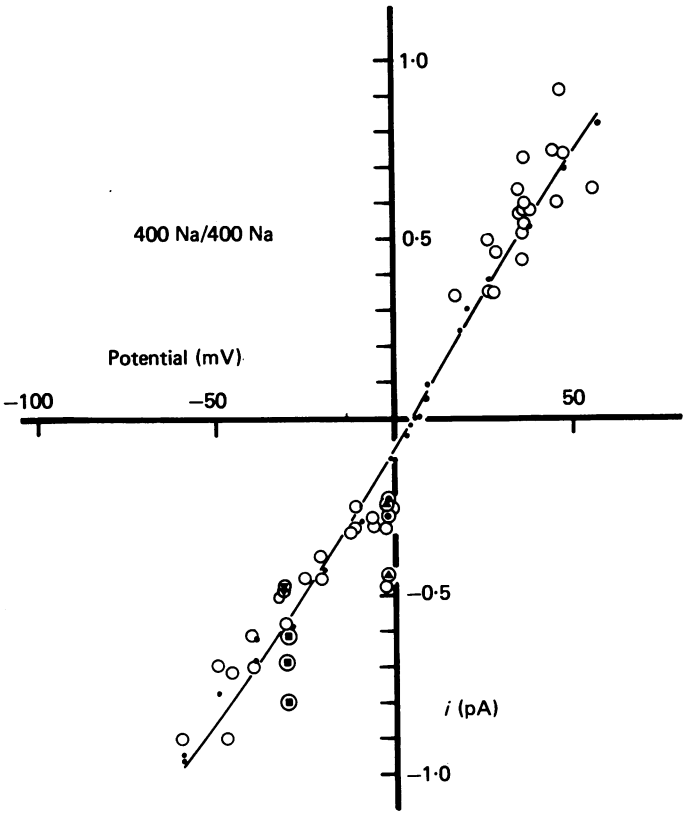

Fig. 5. Unitary currents (open and enclosed symbols) and instantaneous currents (.) plotted against membrane potential in 400 mM-Na sea water with 400 mM-Na intracellular perfusate. The instantaneous currents were multiplied by $2{\cdot}89 \times 10^{-5}$, and the reversal potential was +5 mV. Different enclosed symbols indicate unitary currents from different eggs. They were measured with a 1 sec prepulse to between −80 and −56 mV, and one of them (▲, smaller value) was measured without a prepulse. The peak inward currents changed 3·45-fold (◉), 5·0-fold (▲), 3·92-fold (▼), and 2·7-fold (■).

in 100 Na/400 K were calculated using the inward unitary Na currents. The permeability coefficient estimated from the outward unitary currents was 4·6 times larger ($5{\cdot}28 \times 10^{-1}$ cm^3 sec^{-1}). Probably the background variance was not subtracted satisfactorily because of the small signal-to-noise ratio in the small outward unitary currents in 400 mM-K intracellular perfusate.

E_{Na} was +5 mV in 400 mM-Na sea water with 400 mM-Na intracellular medium. Since the small driving force leads to greater errors in the estimation of the conductance, unitary currents recorded at potentials within ±15 mV from E_{Na} were not used in the calculation of unitary conductances and permeabilities.

Effects of steady-state inactivation upon the unitary currents. The filled symbols in Figs. 4 and 5 show the unitary currents estimated from the Na currents elicited after conditioning prepulses of 1 sec duration to potentials between −80 and −52·5 mV and from one record without prepulse. Slight changes in the unitary currents were observed in two eggs (Fig. 5, ■ and ▲), but the other three eggs (Figs, 4, 5) showed almost constant unitary currents, while the peak inward currents varied by factors of more than 3.

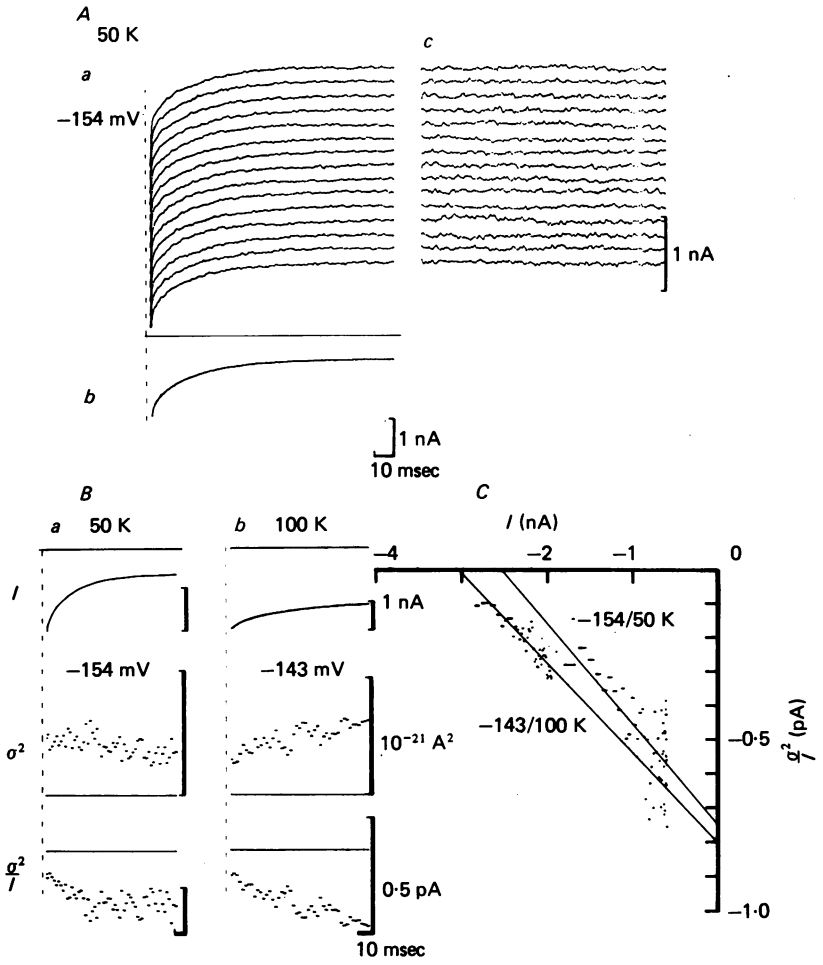

Fig. 6. Transient K inward currents through the anomalous rectifier elicited by clamp pulses to −154 or −143 mV. *A*, fifteen traces of K inward currents in 50 mM-K sea water (*a*), the point-by-point mean of *a* (*b*), and the difference between the records in *a* and the mean (*c*). Currents were low-pass filtered at 0·2 kHz and were sampled at 500 μsec intervals starting 3 msec after the beginning of pulse. *B*, the mean (I), the variance (σ^2) and the ratio (σ^2/I) calculated from eighty records in *a* and from ninety-six records in *b*. Analysis of data started 4 msec after the beginning of the pulse in *a* and *b*. *Ba* is calculated from the same series as in *A*. The background variance ($3{\cdot}97 \times 10^{-22}$ A² for *a* and $1{\cdot}46 \times 10^{-22}$ A² for *b*) was subtracted. *C*, plot of σ^2/I against I presented in *B*. The superimposed lines were drawn from least-squares fits using eqn. (4); the regression coefficient was 0·5 for 50 mM-K and 0·8 for 100 mM-K sea water.

Part II. Anomalous rectifier

Based on several lines of evidence, I have seen that the noise calculated from the transient Na currents may be traced to fluctuations in the state of the Na channels. In order to compare the data obtained by this transient noise method with the data obtained from a completely independent method, I have studied the transient current noise in the inward currents through the anomalous rectifier. The unitary

conductance and the density of anomalous rectifier channels have already been estimated from analysis of steady-state inward current fluctuations through this channel (Ohmori, 1978).

Transient current noise of the anomalous rectifier. In response to a negative test pulse from the zero-current holding potential, a K inward current flows under voltage clamp conditions. After the capacitative transient, a fast activation and a subsequent slow inactivation are observed (Ohmori, 1978). Fig. 6*A*, *a* shows traces of transient K inward currents elicited by step changes of membrane potential to −154 mV in 50 mM-K sea water with Cl-perfusate (In-*c*); after the capacitative transient, the current was sampled at 500 μsec intervals. The mean inward current was calculated (Fig. 6*A*, *b*) and the difference between each current trace and the mean current shows the fluctuations at this potential (Fig. 6*A*, *c*). Fig. 6*B*, *a* illustrates the mean inward current and the variance records calculated from eighty current traces consisting of five groups. The transient component of the point-by-point ratio calculated from this mean inward current and the variance was the mirror image of the transient component of the mean current. In 100 mM-K sea water, inactivation was slower; therefore, a steady-state was not reached within the recording time (Fig. 6*B*, *b*). Even so, the transient component of the ratio between the variance and the mean inward current was the mirror image of the transient component of the mean current estimated from ninety-six records consisting of six groups. Therefore, this transient current noise could be related to the random opening-closing kinetics of the anomalous rectifier. By using eqn. (4), the unitary current, i, and the number of channels, N, were estimated by linear regression analysis. The relation between the mean current and the ratio was plotted in Fig. 6*C*, from recordings in Fig. 6*B*. The superimposed lines were calculated by least-squares fits. The unitary current was −0·75 pA in 50 mM-K sea water at −154 mV and −0·80 pA in 100 mM-K sea water at −143 mV. The number of channels was 3400 for 50 mM-K sea water and 3800 for 100 mM-K sea water.

Fig. 7 shows records in 50 mM-K and in 100 mM-K sea water. In both cases, the slopes of the regression line changed slightly from record to record, but no systematic potential dependence was observed. The mean number of channels was 4100 in 50 mM-K and 4000 in 100 mM-K sea water (see Table 2, K inward currents).

Membrane potential dependence of unitary currents. Previous work on the egg anomalous rectifier (Ohmori, 1978) showed that activation is very fast and that the activation gate is open with probability one in the steady-state at large negative membrane potentials; the inactivation gate is open with probability one in the steady-state at the holding potential. Therefore, zero-time extrapolation of the falling phase of the inward current yields the maximum conductance of the anomalous rectifier, which corresponds to the instantaneous currents of the Na channel, and must be the macroscopic indicator of the unitary current through the single anomalous rectifier channel. Such zero-time extrapolated currents (arrows in Fig. 8*A*) were plotted against membrane potential for 50 mM-K and 100 mM-K sea water, after appropriate normalization (small dots in Fig. 8*B*).

The unitary currents estimated from the transient current noise are given in the same Figure: ○, unitary currents in 50 mM-K sea water; and ●, in 100 mM-K sea water. Fig. 8*B* shows the parallel dependence on the membrane potential of the

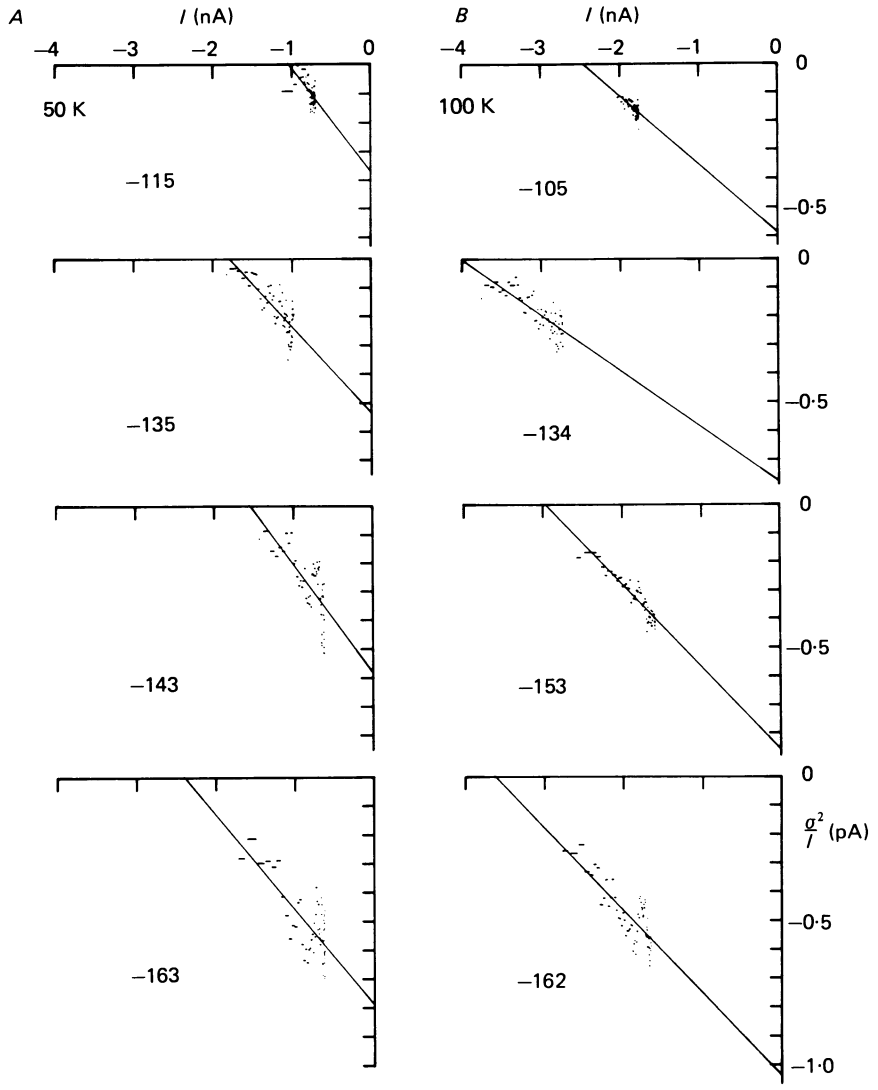

Fig. 7. Plots of σ^2/I against I calculated from the K inward currents through the anomalous rectifier. The mean and variance were obtained from sixty-four to ninety-six current traces low-pass filtered at 0·2 kHz and sampled at 500 μsec intervals.

unitary currents and the zero-time extrapolated currents. The unitary current in 100 mM-K sea water was clearly larger than that in 50 mM-K sea water.

The unitary conductances estimated from Fig. 8*B* were 5·5 pmho in 50 mM-K and 6·92 pmho in 100 mM-K sea water (see Table 2, K inward currents). These values are similar to the unitary conductances previously estimated from the steady-state current noise: 5·97 pmho in 50 mM-K and 8·37 pmho in 100 mM-K sea water (Ohmori, 1978).

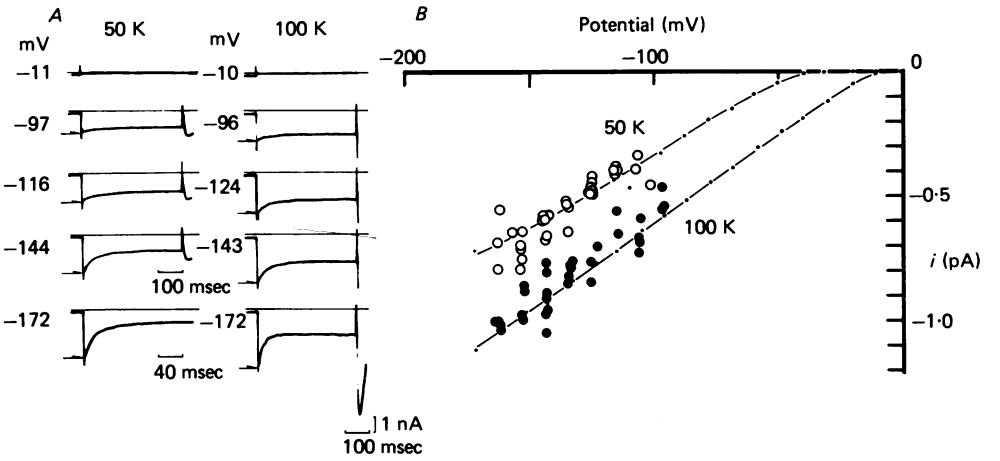

Fig. 8. *A*, *K* inward currents in 50 or in 100 mM-K sea water recorded from two eggs. Arrows indicate the zero-time extrapolated values of the falling phase of the inward currents. These values are plotted as dots in *B*, after multiplication by $2{\cdot}17 \times 10^{-4}$ for 50 mM-K and $3{\cdot}03 \times 10^{-4}$ for 100 mM-K sea water. *B*, unitary currents in 50 mM-K (○) and in 100 mM-K sea water (●), and zero-time-extrapolated currents (small dots) plotted against membrane potential. At potentials where no inactivation occurred the maximum inward currents were plotted instead of the zero-time-extrapolated values.

DISCUSSION

The transient current noise originates from random transitions between states of the Na or of the anomalous rectifier channels of the tunicate egg cell membrane. This conclusion is based upon the following seven arguments. (1) The variance was not a monotonically increasing function of the mean current magnitude, and even decreased at the peak of the mean current (Figs. 2, 6). Especially in 100 mM-K sea water, the variance and the mean K inward current at -143 mV showed a reversed time course (Fig. 6*B*, *b*). Therefore, the variance calculated from the transient currents is not generated by parameters which affect the amount of current flow. (2) The transient component of the point-by-point ratio between the variance and the mean current was the mirror image of the transient component of the mean current itself (Figs. 2*A*, *B*, 6*B*). This is a necessary condition for the underlying stochastic process of random transitions between open and closed states of independent channels. Therefore, the unitary current and the number of channels could be calculated by regression analysis (3) The unitary currents showed a membrane potential dependence almost parallel to that of the instantaneous currents recorded immediately after the peak Na inward currents or to that of the zero-time extrapolated values of the K inward currents. After scaling, the instantaneous (or zero-time extrapolated) current-voltage relation superimposed satisfactorily upon the unitary current-voltage relation (Figs. 4, 5, 8). (4) When $[Na]_o$ or $[Na]_i$ were changed, the changes in the unitary currents were similar to those of the instantaneous currents. The unitary currents of the anomalous rectifier were also a function of $[K]_o$. Therefore, qualitatively, the calculated unitary currents appear to be the currents through single Na or anomalous rectifier channels. (5) The unitary permeability calculated from the unitary Na

currents gave quantitative support for this conclusion; the unitary permeability was found to be essentially constant ($P_{Na} = 1{\cdot}15 \times 10^{-14}$ cm^3 sec^{-1}), irrespective of the large changes of the unitary conductance produced by changes in $[Na]_o$ or $[Na]_i$ (Table 2). (6) Inactivation of the Na channel did not influence the size of unitary currents (Figs. 4, 5). Finally, (7) the unitary conductance of the anomalous rectifier obtained by the analysis of transient noise (Table 2) agreed with that estimated previously from steady-state current fluctuations (Ohmori, 1978).

Before regression analysis, the background variance at the holding potential was subtracted from each test variance. The procedure is based upon the premise that the noise generated by the fluctuation of the states of channels is independent of the noise observed at the resting condition. For the Na channel noise, the background variance was calculated at a holding potential (about -90 mV) at which the open channel probability, $p(t)$, is almost zero. Thus, the contribution to the whole variance from the fluctuations of the states of Na channels should be negligible. For the anomalous rectifier, the background variance was calculated at a holding potential about equal to E_K. Here also, fluctuation in the currents recorded would be independent of fluctuations in the state of the anomalous rectifier. The background variances calculated were different from cell to cell and between different recording conditions. Errors in the estimation of the background variance seriously disturbed the estimation of unitary currents. One example demonstrated that a 40% decrease in the background variance produced an apparent 24% increase in the unitary current and a 13% decrease in the number of channels. However, the agreement between the unitary conductance of the anomalous rectifier obtained in this paper and that reported previously may justify the present method of background subtraction.

The number of ionic channels per half egg (surface area $1{\cdot}14 \times 10^5$ μm^2) was about 7×10^4 for Na channels and about 4000 for the anomalous rectifier (Table 2). The density is $0{\cdot}60/\mu$m^2 for Na channels and $0{\cdot}035/\mu$m^2 for anomalous rectifier channels. The density of Na channels in nerve fibres is considerably larger: 13–35/μm^2 in the lobster giant axon (Moore, Narahashi & Shaw, 1967; Keynes, Ritchie & Rojas, 1971), 483–553/μm^2 in the squid giant axon (Levinson & Meves, 1975; Conti *et al.* 1975, Keynes & Rojas, 1976), and 1000–2000/μm^2 in the frog myelinated nerve fibre (Conti *et al.* 1976*b*; Sigworth, 1977).

The unitary conductance, γ, estimated for the Na channel is 7·35 pmho in 400 mM-Na sea water with 400 mM-K intracellular medium, and the Na permeability, P_{Na}, of the single Na channel is $1{\cdot}15 \times 10^{-14}$ cm^3 sec^{-1}. Similar values for γ (7·7-8 pmho) and a four times larger value for P_{Na} ($4{\cdot}3 \times 10^{-14}$ cm^3 sec^{-1}) have been found in frog nerve fibres (Conti *et al.* 1976*b*; Sigworth, 1977). The unitary conductance of the anomalous rectifier is of the same order as that of the Na channel (Table 2). With an internal Na concentration of 400 mM (In-*b*), the unitary conductance, γ, in 400 mM-Na sea water was increased to 15·7 pmho. This may be the limiting conductance of this channel and is close to that reported for the ACh sensitive channel of the frog end-plate (Anderson & Stevens, 1973).

It is my great pleasure to acknowledge the help of Professor K. Takahashi. At every stage of the work and during the writing of the paper his advice and the discussions with him were most helpful. I also thank Professors S. Hagiwara and A. Takeuchi for their helpful and valuable criticisms of the manuscript and Drs W. L. Byerly and S. G. Rayport for reading and improving the manuscript.

REFERENCES

ANDERSON, C. R. & STEVENS, C. F. (1973). Voltage clamp analysis of acetylcholine produced end-plate current fluctuations at frog neuromuscular junction. *J. Physiol.* **235**, 655–691.

BENDAT, J. S. & PIERSOL, A. G. (1971). *Random Data. Analysis and Measurement Procedures*. New York: Wiley Interscience.

CONTI, F., DE FELICE, L. J. & WANKE, E. (1975). Potassium and sodium ion current noise in the membrane of the squid giant axon. *J. Physiol.* **248**, 45–82.

CONTI, F., HILLE, B., NEUMCKE, B., NONNER, W. & STÄMPFLI, R. (1976*a*). Measurement of the conductance of the sodium channel from current fluctuations at the node of Ranvier. *J. Physiol.* **262**, 699–727.

CONTI, F., HILLE, B., NEUMCKE, B., NONNER, W. & STÄMPFLI, R. (1976*b*) Conductance of the sodium channel in myelinated nerve fibres with modified sodium inactivation. *J. Physiol.* **262**, 729–742.

GOLDMAN, D. E. (1943). Potential, impedance, and rectification in membranes. *J. gen. Physiol.* **27**, 37–60.

HAGIWARA, S. & YOSHII, M. (1979). Effects of internal potassium and sodium on the anomalous rectification of the starfish egg as examined by internal perfusion. *J. Physiol.* **292**, 251–265.

HODGKIN, A. L. & HUXLEY, A. F. (1952). A quantitative description of membrane currents and its application to conduction and excitation in nerve. *J. Physiol.* **117**, 500–544.

HODGKIN, A. L. & KATZ, B. (1949). The effect of sodium ions on the electrical activity of the giant axon of the squid. *J. Physiol.* **108**, 37–77.

KATZ, B. & MILEDI, R. (1972). The statistical nature of the acetylcholine potential and its molecular components. *J. Physiol.* **224**, 665–699.

KEYNES, R. D., RITCHIE, J. M. & ROJAS, E. (1971). The binding of tetrodotoxin to nerve membranes. *J. Physiol.* **213**, 235–254.

KEYNES, R. D. & ROJAS, E. (1976). The temporal and steady-state relationships between activation of the sodium conductance and movement of the gating particles in the squid giant axon. *J. Physiol.* **255**, 157–189.

LEVINSON, S. R. & MEVES, H. (1975). The binding of tritiated tetrodotoxin to squid giant axons. *Phil. Trans. R. Soc.* B **270**, 349–352.

MOORE, J. W., NARAHASHI, T. & SHAW, T. I. (1967). An upper limit to the number of sodium channels in nerve membrane? *J. Physiol.* **188**, 99–105.

NEHER, E. & STEVENS, C. F. (1977). Conductance fluctuations and ionic pores in membranes. *A. Rev. Biophys. Bioeng.* **6**, 348–381.

OHMORI H. (1978). Inactivation kinetics and steady-state current noise in the anomalous rectifier of tunicate egg cell membranes. *J. Physiol.* **281**, 77–99.

OKAMOTO, H., TAKAHASHI, K. & YOSHII, M. (1976). Membrane currents of the tunicate egg under the voltage-clamp condition. *J. Physiol.* **254**, 607–638.

SIGWORTH, F. J. (1977). Sodium channels in nerve apparently have two conductance states. *Nature, Lond.* **270**, 265–267.

TAKAHASHI, K. & YOSHII, M. (1978). Effects of internal free calcium upon the sodium and calcium channels in the tunicate egg analyzed by the internal perfusion technique. *J. Physiol.* **279**, 519–549.